

# Modeling Imatinib-Treated Chronic Myelogenous Leukemia

**Cara Peters**

[cpeters3@math.umd.edu](mailto:cpeters3@math.umd.edu)

**Advisor: Dr. Doron Levy**

[dlevy@math.umd.edu](mailto:dlevy@math.umd.edu)

Department of Mathematics

Center for Scientific Computing and Mathematical Modeling

## **Abstract**

Chronic Myelogenous Leukemia (CML) is a blood cancer affecting approximately 1 in 100,000 people. While there are many different treatments for controlling CML, there is currently no cure. Recently, many mathematical models have been developed to explore disease genesis and the effects of various therapies with the hope of improving or discovering new therapeutic strategies. It will be the goal of this project to study three such models: an agent-based model, a system of difference equations and a system of partial differential equations.

# 1 Project Background

Chronic Myelogenous Leukemia (CML) is a type of blood cancer resulting in the overproduction of white blood cells. Approximately 20% of all leukemia cases are CML. CML can be characterized by a genetic mutation in hematopoietic stem cells in which a translocation between chromosomes 9 and 22 occurs. During this translocation, fusion of the bcr-abl gene occurs on chromosome 22 to form what is known as the Philadelphia (Ph) chromosome, a detectable characteristic in 90% of all CML patients. Fusion of this gene results in increased tyrosine kinase activity contributing to uncontrolled stem cell growth and survival, and ultimately cancer.

There are currently many types of treatment available to CML patients. Of particular interest is a form of targeted therapy involving the drug Imatinib. Imatinib is a tyrosine kinase inhibitor that specifically targets Ph<sup>+</sup> cells and binds to the bcr-abl enzyme. This drug controls the population of cancer cells in two ways: by preventing proliferation of mutated cells and increasing apoptosis or cellular suicide. Although quite effective as a control, Imatinib is not a cure for CML.

In the past decade, there has been much interest in the use of mathematical models to gain further insight into the dynamics of CML genesis and explore the effects of treatment. This project will consider three such models, each biologically based on the same cell differentiation process as described by Roeder *et al.* This process consists of three stages of cell differentiation: stem cells, precursors and mature cells. Additionally, stem cells are categorized as either non-proliferating ( $A$ ) or proliferating cells ( $\Omega$ ). Movement between compartments is as follows (fig. 1).

Each stem cell may be characterized by its cellular affinity, a quantity based on cell age and state. Cells in  $A$  increase their affinity over time until the maximum affinity is reached. They transfer from  $A$  to  $\Omega$  with probability  $\omega$  determined by affinity and the total number of proliferating cells. In  $\Omega$ , stem cells proliferate by completing the 48 hour cell cycle. The cell cycle consists of four necessary phases for cell growth and division. These stages in order are  $G_1$ ,  $S$ ,  $G_2$ , and  $M$ . Cells enter  $\Omega$  from  $A$  at hour 32 of the cell cycle, the beginning of the  $S$  phase during which DNA synthesis occurs. At hour 48, the cell divides into two daughter cells that each begin the cycle in the  $G_1$  growth phase. Transitions from  $\Omega$  to  $A$  occur during the  $G_1$  phase with probability  $\alpha$ . Cell affinity decreases over time in  $\Omega$  until the minimum affinity is attained.

Stem cells with minimum affinity differentiate into precursor cells. These cells divide once every 24 hours for 20 days, at which point they become mature cells. Cells live in the mature stage for 8 days before dying.

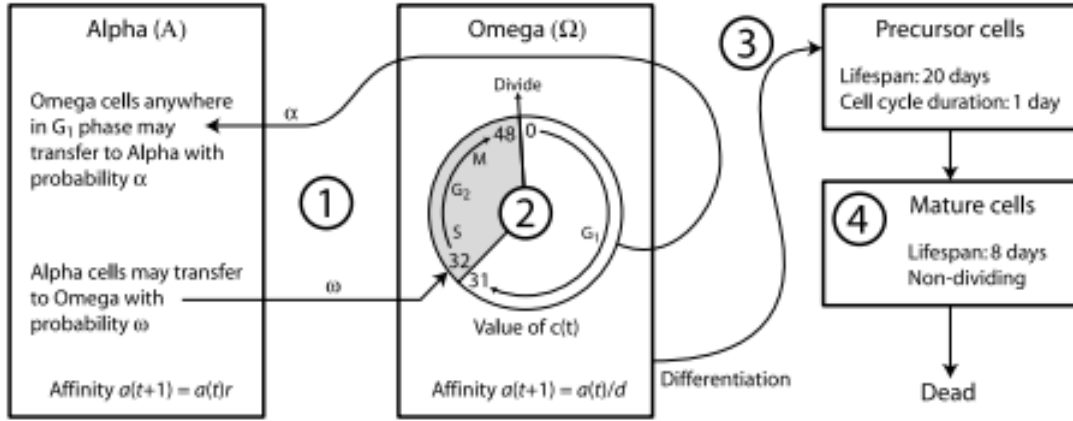


**Figure 1:** A cell state diagram as proposed by Roeder *et al.* Figure from [2].

The biology described here is a simplification of the cell maturation process and makes a few assumptions. Firstly, the differentiation process has been reduced to three stages of maturation. Second, transition probabilities between stem cell compartments are assumed to be based on affinity, an internal quantity for each stem cell that varies in time within an interval  $[a_{min}, a_{max}]$ . Affinity is a notion whose existence was postulated by Roeder [1] and is not directly associated with any known biological mechanism specific to the hematopoietic system. Furthermore, the time spent in each stage is deterministic. It is assumed that these lifespans are known and fixed.

## 2 Approach

There will be three components to this project. The first is to implement an agent based model (ABM) for describing CML genesis as described by Roeder *et al.* The second component will be to implement a reformulation of this model as a system of discretized difference equations [2]. Lastly, a system of PDEs will be used to simulate CML and its treatment [3]. All three algorithms are based upon the same underlying biological model (fig. 1) and use the same parameter values as given by Roeder.

### 2.1 Agent Based Model

Roeder's agent based model simulates each cell individually according to a set of rules (fig. 2). At each discrete time step (1 hour) these rules are applied and cells are updated simultaneously. At the start of each time step, the number of cells in the  $A$  and  $\Omega$  compartments is determined and used to govern the movement of each cell in the model. As previously mentioned, cells in  $A$  transition to  $\Omega$  with probability  $\omega$ , while cells in  $\Omega$  move to  $A$  with probability  $\alpha$ .

$$\begin{aligned}\omega(\Omega(t), a(t)) &= \frac{a_{min}}{a(t)} f_{\omega}(\Omega(t)) \\ \alpha(\Omega(t), a(t)) &= \frac{a(t)}{a_{max}} f_{\alpha}(A(t))\end{aligned}\quad (1)$$

The transition probabilities are dependent on the affinity  $a(t)$  as well as the number of non-proliferating cells  $A(t)$  and proliferating cells  $\Omega(t)$ . The functions  $f_\omega$  and  $f_\alpha$  are sigmoidal functions.



**Figure 2:** Update algorithm for ABM. Cell affinity is given by  $a(t)$ , position in cell cycle by  $c(t)$  and cell compartment by  $m(t)$ .  $\Delta t = 1 \text{ hr}$ . From [1].

Cells that remain in A increase affinity by a factor  $r$  known as the regeneration factor. When cells transfer into  $\Omega$ ,  $c(t)$  is set to correspond to the beginning of the S phase of the cell cycle. Cells remaining in  $\Omega$ , may only transition to A when  $c(t)$  corresponds to the G<sub>1</sub> phase. Once the cell cycle has been completed, the cell duplicates. Affinity of  $\Omega$  cells is decreased by a differentiation factor  $1/d$  until minimum affinity is reached. Once minimum affinity has been reached, the cell begins terminal differentiation.

This model can become quite computationally complex, as it is based on the number of cells being simulated. At initial implementation by Roeder in 2006, simulations of approximately  $10^5$  cells were achieved. This is only about  $\frac{1}{10}$  of realistic values seen in patients.

### 2.1.1 Simulation of CML Genesis

The algorithm depicted in figure 2 demonstrates the rules for updating healthy or nonleukemic cells. To simulate the onset of CML in healthy patient and track disease genesis, the sigmoidal functions  $f_\omega$  and  $f_\alpha$  will be altered with parameters specific to  $\text{Ph}^+$  cells, for a single cell in a population of  $\text{Ph}^-$  cells. That cell will be labeled leukemic ( $\text{Ph}^+$ ) and tracked over time. All of its progeny will be considered as  $\text{Ph}^+$  cells.

### 2.1.2 Simulation of Treatment

Treatment is introduced to the algorithm in two ways, reflecting the two ways Imatinib can affect  $\text{Ph}^+$  cells. First, Imatinib can limit proliferation of mutated cells. This will be accomplished in the model by altering the  $f_\omega$  function for previously unaffected  $\text{Ph}^+$  cells with probability  $r_{inh}$  at each time step. Once this change has been made, these cells will be marked as affected ( $\text{Ph}^+$ ) and maintain this configuration of  $\omega$  for the duration of the simulation. Altering this function alone decreases the ability for resting to cells to transition to  $\Omega$  and begin proliferating. Imatinib also increases apoptotic activity in  $\text{Ph}^+$  cells. Implementation of this function will consist of removing  $\text{Ph}^+$  cells in  $\Omega$  from the system with probability  $r_{deg}$  at each time step.

Simulation of Imatinib treatment will begin once the proportion of differentiated  $\text{Ph}^+$  cells has reached more than 99.5%. To stop treatment, all parameter values and functions are reset to their initial values.

## 2.2 A System of Difference Equations Model

The second model will replace the ABM with a system of discretized difference equations. Rather than simulating each cell individually, the system will group cells by their common characteristics i.e., cell state compartment, affinity level, cell cycle position. The progression of CML can be simulated by tracking the number of cells in each group. This approach reduces computational complexity of the model and allows for simulation of more realistic cell numbers.

In order to formulate the difference equations, the state space must be discretized. Time is already discretized in the ABM; cell positions are updated at fixed time steps of one hour. Affinity is discretized by setting  $a(t) = e^{-k\rho}$  where  $\rho = 0.0488$  and  $0 \leq k \leq 127$ . The affinity of each cell can now be characterized discretely by the value of  $k$  where  $\log(a(t)) = -k\rho$ .

### 2.2.1 The Difference Equations

The stem cell populations can be represented by the following difference equations with  $k$  representing cell affinity and  $c$  representing position in the cell cycle:

$$A_k(t+1) = \begin{cases} (A_0(t) - B_0(t)) + (A_1(t) - B_1(t)) + (A_2(t) - B_2(t)), & k = 0 \\ (A_{k+2}(t) - B_{k+2}(t)) + \sum_{c=0}^{31} \Psi_{k,c}(t), & k = 1, \dots, 125 \\ \sum_{c=0}^{31} \Psi_{k,c}(t), & k = 126, 127 \end{cases} \quad (2)$$

$$\Omega_k(t+1) = \begin{cases} B_0(t), & k=0, c=32 \\ 2\Omega_{k-1,48}(t), & k>0, c=0 \\ \Omega_{k-1,c-1}(t) - \Psi_{k-1,c-1}(t), & k>0, c=1, \dots, 31 \\ \left(\Omega_{k-1,31}(t) - \Psi_{k-1,31}(t)\right) + B_k(t), & k>0, c=32 \\ \Omega_{k-1,c-1}(t), & k>0, c=33, \dots, 48 \\ 0 & \text{otherwise} \end{cases} \quad (3)$$

Transitions between the  $A_k$  and  $\Omega_{k,c}$  compartments are determined by the binomial random variables  $B_k$  and  $\Psi_{k,c}$  which have the following distributions:

$$B_k(t) \sim \text{Bin}\left(A_k(t), \omega(\Omega(t), e^{-k\rho})\right)$$

$$\Psi_{k,c}(t) \sim \text{Bin}\left(\Omega_{k,c}(t), \alpha(A(t), e^{-k\rho})\right), \quad c = 0, \dots, 31$$

Here  $\Omega(t)$  and  $A(t)$  denote the total number of proliferating and resting cells respectively, and are found by summing over all values of  $k$  and  $c$ . The transition probabilities  $\omega$  and  $\alpha$  are as previously given by (1).

The differentiated cells can be represented in a similar fashion. The equations for precursors are denoted by  $P_j(t)$  where  $j = 0, \dots, 479$  is the number of hours a cell has spent in this compartment, up to 20 days. Similarly mature cells are denoted by  $M_j(t)$  where  $j = 0, \dots, 191$  is the number of hours spent as a mature cell, up to 8 days.

$$P_j(t+1) = \begin{cases} \sum_{c=0}^{48} \Omega_{127,c}(t) - \sum_{c=0}^{31} \Psi_{127,c}(t), & j=0 \\ 2P_{j-1}(t), & j=24, 48, 72, \dots, 456 \\ P_{j-1}(t), & \text{otherwise} \end{cases} \quad (4)$$

$$M_j(t+1) = \begin{cases} 2P_{479}(t), & j=0 \\ M_{j-1}(t), & \text{otherwise} \end{cases} \quad (5)$$

These equations directly reflect the rules of cell differentiation as presented in the cell state diagram (fig. 1). The first line of (4) represents proliferating cells that have attained minimum affinity and differentiate into precursors. Precursors divide every 24 hours, producing two daughter cells, as represented by line two. Line three denotes an increase in age, which is necessary to track the time spent as a precursor before maturing. The first line of (5) signifies the number of precursors that undergo one final division before entering the mature state. Similar to the final line of (4), the second line of (5) tracks the age of mature cells before they die.

### 2.2.2 Modeling CML and Imatinib Treatment

Equations (2) to (5) as written will be used to simulate  $\text{Ph}^-$  cells. As with ABM, alterations to some of these equations will need to be made in order to represent  $\text{Ph}^+$  cells and Imatinib-affected cells ( $\text{Ph}^{+/A}$ ).

Ph<sup>+</sup> cells uncontrollably proliferate and so the transition rates between A and  $\Omega$  differ from those of Ph<sup>-</sup> cells. The transition functions  $f_\omega$  and  $f_\alpha$  are updated with new parameter values that correspond to Ph<sup>+</sup> cells. This is the only update necessary to simulate CML genesis. Further changes to the Ph<sup>+</sup> equations are necessary when Imatinib is introduced. When the drug is introduced, proliferating stem cells become Imatinib affected with probability  $r_{inh}$  at each time step. This probability is given by  $\Omega^{+/I}(t) \sim Bin(\Omega_{k,c}^+(t), r_{inh})$  where  $\Omega^{+/I}(t)$  represents proliferating Ph<sup>+</sup> stem cells that become affected at time  $t$ . These cells will be removed from the Ph<sup>+</sup> cell population at the beginning of each time step before any other transition occurs. To accomplish this,  $\Omega_{k,c}^+(t + 1)$  from (3) will change to become the number of cells remaining unaffected for the next time step. This is given by  $\Omega_{k,c}^{+/R}(t) = \Omega_{k,c}^+(t) - \Omega_{k,c}^{+/I}(t)$ .

The Ph<sup>+A</sup> cell population is also governed by slightly altered equations. First, since Imatinib inhibits the ability of these cells to proliferate, transition functions  $f_\omega$  and  $f_\alpha$  will be updated with corresponding parameter values. Second, affected proliferating stem cells,  $\Omega^{+/A}$  undergo apoptosis at each time step with probability  $r_{deg}$ . These cells will be removed at the beginning of each time step, before regular transitions occur.

## 2.3 A PDE Model

The third model transforms Roeder's ABM into a system of partial differential equations, the goal being to describe the same CML dynamics with continuous variables. The PDE model has advantages over the original model. Like the system of difference equations, it reduces the complexity of ABM, which can produce a solution in less time and allows simulations of realistic cell population sizes. Additionally, it tracks disease genesis in continuous time which more accurately reflects true biological processes.

Transitions for stem cells will be governed by three variables  $t$ ,  $a$  and  $c$ , which can be thought of as three internal clocks representing real time, affinity and cell cycle position respectively. Differentiated cells are not dependent on affinity or the cell cycle. Lifespans and functions of these cells will be represented by  $t$  and  $s$ , where  $s$  denotes cell age.

### 2.3.1 The System and Boundary Conditions

As noted in the difference equation model, the log of cell affinity is linear with respect to real time. Hence, the population of non-proliferating cells A will be denoted  $A(x, t)$  where  $x = -\log(a)$  with  $a$  being affinity. Over time, cells in A increase their affinity up to some maximum value. This will correspond to  $x_{min} = -\log(a_{max})$ . To deal with the accumulation of cells occurring at this boundary, cells with maximum affinity will be considered as a subpopulation denoted  $A^*(t)$ . The population of proliferating cells will be denoted  $\Omega(x, c, t)$ . Additionally,  $\Omega^*(x, t)$  will be used to denote the subpopulation of proliferating cells that transferred into  $\Omega$  from  $A^*$ .

The PDEs for these four subpopulations are as follows:

$$\frac{\partial A}{\partial t} - \rho_r \frac{\partial A}{\partial t} = -\omega(\bar{\Omega}, e^{-x})A + \alpha(\bar{A}, e^{-x}) \int_0^{32} \Omega(x, c, t) dc + \begin{cases} 0, & x \in X_a \\ \alpha(\bar{A}, e^{-x})\Omega^*, & x \in X_b \end{cases} \quad (6)$$

$$\frac{dA^*}{dt} = \rho_r A(x_{min}, t) - \omega(\bar{\Omega}, e^{-x_{min}})A^* \quad (7)$$

$$\frac{\partial \Omega}{\partial t} + \rho_d \frac{\partial \Omega}{\partial x} + \frac{\partial \Omega}{\partial c} = \begin{cases} -\alpha(\bar{A}, e^{-x})\Omega, & \text{for } c \in (0, 32] \\ 0, & \text{for } c \in (32, 49] \end{cases} \quad (8)$$

$$\frac{\partial \Omega^*}{\partial t} + \rho_d \frac{\partial \Omega^*}{\partial x} = \begin{cases} 0, & x \in X_a \\ -\alpha(\bar{A}, e^{-x})\Omega^*, & x \in X_b \end{cases} \quad (9)$$

The domain of  $x$  is divided into two subsets  $X_a$  and  $X_b$  where  $X_a = (x_{min}, y_1] \cup (y_2, y_3] \cup (y_4, y_5]$  and  $X_b = (y_1, y_2] \cup (y_3, y_4] \cup (y_5, x_{max}]$ , with  $y_1, y_2, y_3, y_4$ , and  $y_5$  being constants corresponding to affinity values at which  $\Omega^*$  cells reach cell cycle time counters of 49, 32, 49, 32, and 49 respectively [3]. The transition probabilities  $\omega$  and  $\alpha$  are given by (1). Regeneration and differentiation factors for affinity are incorporated into the advection rates  $\rho_r = \log r$  and  $\rho_d = \log d$ . Equations (6) - (9) are dependent on the total population of cells in A and  $\Omega$ . These are denoted by

$$\bar{A}(t) = \int_{x_{min}}^{x_{max}} A(x, t) dx + A^*(t)$$

$$\bar{\Omega}(t) = \int_{x_{min}}^{x_{max}} \int_0^{49} \Omega(x, c, t) dc dx + \int_{x_{min}}^{x_{max}} \Omega^*(x, t) dx$$

Boundary conditions for A and  $\Omega$  are given by

$$\begin{aligned} A(x_{min}, t) &= 0 \\ \Omega(x, 0, t) &= 2\Omega(x, 49, t) \\ \Omega(x, 32^+, t) &= \Omega(x, 32^-, t) + \omega(\bar{\Omega}, e^{-x})A \\ \Omega^*(x_{min}, t) &= \frac{\omega(\bar{\Omega}, e^{-x_{min}})}{\rho_d} A^* \\ \Omega(y_i^+, t) &= 2\Omega(y_i^-, t), \quad i = 1, 3, 5 \end{aligned} \quad (10)$$

Cells that have attained minimum affinity differentiate into precursor cells, where their behavior is no longer dependent on affinity or the cell cycle seen in  $\Omega$ . The PDE for these cells can then be written as a linear advection equation based on age:

$$\frac{\partial P}{\partial t} + \frac{\partial P}{\partial s} = 0, \quad s \in [0, 480) \quad (11)$$

Precursors divide once every 24 hours. This will be incorporated into the boundary conditions for (11) which are given as

$$\begin{cases} P(0, t) = \rho_d \left( \int_0^{32} \Omega(x_{max}, c, t) dc + \Omega^*(x_{max}, t) \right) \\ P(v^+, t) = 2P(v^-, t), \quad v = 24, 48, 72, \dots, 456 \end{cases} \quad (12)$$

Here, the boundaries are considered to be the times at which division occurs. Mature cells can be considered in a similar fashion, as their population depends only on real time and cell age. The PDE is given by (13) with boundary condition (14) to signify the final division of precursor cells.

$$\frac{\partial M}{\partial t} + \frac{\partial M}{\partial s} = 0, \quad s \in [0, 192) \quad (13)$$

$$M(0, t) = 2P(480, t) \quad (14)$$

### 2.3.2 Modeling CML and Imatinib Treatment

Simulating disease genesis and treatment in the PDE model will be similar as in the difference equations. Leukemic cells will be denoted by  $\text{Ph}^+$ , nonleukemic cells as  $\text{Ph}^-$  and Imatinib-affected leukemic cells by  $\text{Ph}^{+/A}$ . A separate set of PDEs will be formulated for each population according to equations (6) - (9), (11) and (13), with some modifications for  $\text{Ph}^+$  and  $\text{Ph}^{+/A}$  cells. The boundary conditions will remain the same across all populations. PDEs for  $\text{Ph}^-$  cells are as written above.

Unaffected  $\text{Ph}^+$  cells transition between A and  $\Omega$  based on transition functions  $f_{\alpha/\omega}$ , with parameter values specific to  $\text{Ph}^+$  cells. Proliferating leukemic cells  $\Omega^+$  can become Imatinib affected or undergo apoptosis. This is introduced in by altering (8) and (9) to include an additional term on the right hand side:  $-(r_{inh} + r_{deg})\Omega^+$  and  $-(r_{inh} + r_{deg})\Omega^{*,+}$  respectively.

Imatinib-affected cells transition between A and  $\Omega$  based on transition functions  $f_{\alpha/\omega}$ , with parameter values specific to  $\text{Ph}^{+/A}$  cells. The drug effects are introduced by including an additional right hand side term to (8) and (9) of the form  $r_{inh}\Omega^+ - r_{deg}\Omega^i$  and  $r_{inh}\Omega^{*,+} - r_{deg}\Omega^{*,i}$  respectively. Here  $\Omega^i$  denotes the affected proliferating stem cell population.

### 2.3.3 Numerical Methods

To numerically simulate the PDE model, first the domain will be discretized into an equally spaced grid. The equations and boundary conditions given above will be discretized using the numerical scheme presented by Kim *et al.* Starting with the stem cells, the grid points for the domain  $[x_{min}, x_{max}] \times [0, 49] \times \mathbb{R}_0^+$  are given by  $x_j = j\Delta x$ ,  $c_k = k\Delta c$  and  $t_n = n\Delta t$ , where

$$\Delta x = \frac{x_{max} - x_{min}}{J}, \quad \Delta c = \frac{49}{K}$$

and  $j = 0, \dots, J$ ,  $k = 0, \dots, K$ , and  $n = 0, \dots, N$ . Let  $\lambda_x = \Delta t/\Delta x$  be the fixed mesh ratio. The composite trapezoidal rule will be used to evaluate all integrals that appear in the above equations and is denoted by  $\mathcal{T}_u(f) = \frac{\Delta u}{2} \sum_{l=0}^{M-1} (f(u_{l+1}) - f(u_l))$ . Note that  $\hat{A}_n, \hat{\Omega}_n, \tilde{A}_{j,n}, \tilde{A}_n^*$ ,  $\tilde{\Omega}_{j,k,n}$  and  $\tilde{\Omega}_{j,n}^*$  will represent the numerical approximations for  $\bar{A}(t_n), \bar{\Omega}(t_n), A(x_j, t_n), A^*(t_n), \Omega(x_j, c_k, t_n)$  and  $\Omega^*(x_j, t_n)$  respectively. Following this notation,

$$\begin{aligned} \hat{A}_n &= \mathcal{T}_x(\tilde{A}_{-,n}) + \tilde{A}_n^* \\ \hat{\Omega}_n &= \mathcal{T}_x \circ \mathcal{T}_c(\tilde{\Omega}_{-,-,n}) + \mathcal{T}_x(\tilde{\Omega}_{-,n}^*) \end{aligned}$$

Then the numerical approximation for (6) is

$$\begin{aligned}\tilde{A}_{j,n+1} = & \tilde{A}_{j,n} + \lambda_x \rho_r (\tilde{A}_{j+1,n} - \tilde{A}_{j,n}) - \Delta t (\omega(\hat{\Omega}_n, e^{-x_j}) \tilde{A}_{j,n} + \alpha(\hat{A}_n, e^{-x_j}) \mathcal{T}_c(\tilde{\Omega}_{j,-n})) \\ & + \begin{cases} 0, & x_j \in X_a, \\ (\Delta t) \alpha(\hat{A}_n, e^{-x_j}) \tilde{\Omega}_{j,n}^*, & x_j \in X_b. \end{cases}\end{aligned}$$

with associated boundary condition obtained from the first line of (10)

$$\tilde{A}_{j,n+1} = 0.$$

The approximation for (7) is given as

$$\tilde{A}_{n+1}^* = \tilde{A}_n^* + \Delta t (\rho_r A_{0,n} - \omega(\hat{\Omega}_n, e^{-x_0})) \tilde{A}_n^*.$$

The numerical scheme for  $\Omega$  cells is derived from (8) as

$$\begin{aligned}\tilde{\Omega}_{j,k,n+1} = & \tilde{\Omega}_{j,k,n} + \lambda_x \rho_d (\tilde{\Omega}_{j,k,n} - \tilde{\Omega}_{j-1,k,n}) - \lambda_c (\tilde{\Omega}_{j,k,n} - \tilde{\Omega}_{j,k-1,n}) \\ & + \begin{cases} -(\Delta t) \alpha(\hat{A}_n, e^{-x_j}) \Omega_{j,k,n}, & \text{for } c \in (0, 32], \\ 0, & \text{for } c \in (32, 49]. \end{cases}\end{aligned}$$

with boundary conditions

$$\begin{aligned}\tilde{\Omega}_{0,k,n} &= 0 \quad \forall k, n \\ \tilde{\Omega}_{j,0,n+1} &= 2\tilde{\Omega}_{j,K,n} \\ \tilde{\Omega}_{j,\bar{k}^+,n+1} &= \tilde{\Omega}_{j,\bar{k}^-,n+1} + \omega(\hat{\Omega}_n, e^{-x_j}) \tilde{A}_{j,n+1}.\end{aligned}$$

The first boundary condition corresponds to  $x = x_0$ , the second to  $c = 0$ , and the last to  $c = 32$  where  $\bar{k}$  is the index between 0 and  $K$  such that  $c_{\bar{k}}$  is as close to 32 as possible [3]. Next, equation (9) for cells in  $\Omega^*$  is discretized as

$$\tilde{\Omega}_{j,n+1}^* = \tilde{\Omega}_{j,n}^* - \lambda_x \rho_d (\tilde{\Omega}_{j,n}^* - \tilde{\Omega}_{j-1,n}^*) + \begin{cases} 0, & x_j \in X_a, \\ -(\Delta t) \alpha(\hat{A}_n, e^{-x_j}) \tilde{\Omega}_{j,n}^*, & x_j \in X_b. \end{cases}$$

The boundary condition given by the fourth and fifth lines of (10) become

$$\begin{aligned}\tilde{\Omega}_{0,n+1}^* &= \frac{\omega(\hat{\Omega}_n, e^{-x_0})}{\rho_d} \tilde{A}_n^* \\ \tilde{\Omega}_{j^+,n+1}^* &= 2\tilde{\Omega}_{j^-,n+1}^*.\end{aligned}$$

For the differentiated cells, the grid points for the time domain is the same as stated above. The grid points for the age domains  $[0, 480]$  and  $[0, 192]$  for precursor and mature cells respectively, are given by  $s_i = i\Delta s$  where  $\Delta s = 1/w$  for some integer  $w$  and  $i = 1, \dots, I_m, \dots, I_p$ . Note that  $\tilde{P}$  and  $\tilde{M}$  represent the numerical approximations to  $P$  and  $M$ , respectively. An explicit upwind scheme is used to approximate equations (11) and (13) as

$$\begin{aligned}\tilde{P}_{i,n+1} &= \tilde{P}_{i,n} - \lambda_s (\tilde{P}_{i,n} - \tilde{P}_{i-1,n}) \\ \tilde{M}_{i,n+1} &= \tilde{M}_{i,n} - \lambda_s (\tilde{M}_{i,n} - \tilde{M}_{i-1,n})\end{aligned}$$

The boundary conditions are given as

$$\begin{cases} \tilde{P}_{0,n} = \rho_d (\mathcal{T}_c(\tilde{\Omega}_{j,-n}) + \tilde{\Omega}_{j,n}^*) \\ \tilde{P}_{vw^+,n} = 2\tilde{P}_{vw^-,n} & \text{for } v = 24, 48, 72, \dots, 456 \\ \tilde{M}_{0,n} = 2\tilde{P}_{480,n} \end{cases}$$

The numerical approximations for leukemic cells are derived similarly. This numerical method is a first-order method. Extensions of the scheme in higher-order can be considered as a follow-up project.

### 3 Implementation

All three models will be implemented in Matlab R2014a. Simulations will be run on an ASUS Notebook with a 2.4 GHz Intel Core i5 processor and 8 GB of RAM.

### 4 Validation

As previously mentioned, the complexity of ABM is based on the number of agents in the system. The completed model will be validated by running simulations first on a small number of cells, increasing gradually to larger values. Validity will be determined by comparing resulting cell counts and figures to those presented by Roeder *et al.* This model should be able to produce figures of a similar shape and scale. Furthermore, the ability to simulate total cell count on the order of  $10^5$  or larger will demonstrate an efficient implementation of the ABM. Simulations of the nonleukemic cell population will be run and validated before introducing the algorithm alterations representing CML genesis and Imatinib treatment.

The difference equation model will be validated in a similar fashion as the ABM. Simulations should be able to accurately recover the figures produced by Kim *et al.* Figure 3 shows the number of nonleukemic stem cells by compartment at each level of affinity. For ABM, stem cells are grouped by affinity first and then plotted as a bar chart. The steady state profile for the difference equations is achieved by plotting  $A_k(t_s)$  and  $\sum_c \Omega_{k,c}(t_s)$  versus affinity level  $k$ , where  $t_s$  is the steady state time. Figure 4 depicts the number of mature leukemic ( $M^+(t) = \sum_s M_s^+(t)$ ) and nonleukemic cells ( $M^-(t) = \sum_s M_s^-(t)$ ) versus time. It will be enough to generate similar steady state dynamics with approximately the same cell population values in order to determine validity.

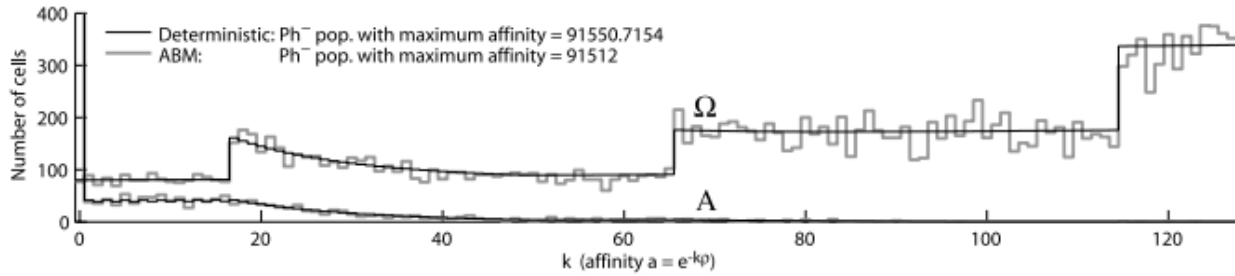


**Figure 3:** Steady state profile for nonleukemic stem cells achieved by ABM and difference equation method. Both resting and proliferating stem cell populations are shown. From [2].

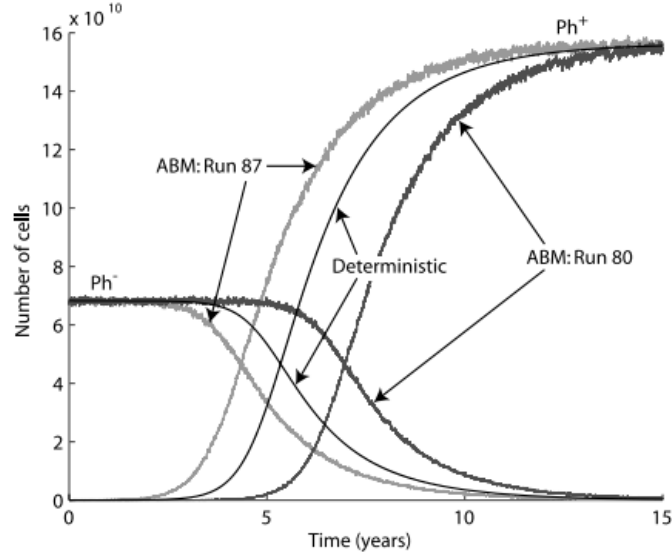


**Figure 4:** Simulation of CML genesis. Dynamics of both leukemic ( $Ph^+$ ) and nonleukemic ( $Ph^-$ ) cells are shown by plotting the number of mature cells in each population versus time. From [2].

Validation of the PDE model will be accomplished in a different manner. It must first be verified that the numerical scheme for the model produces accurate results for the PDE in question. Since the CML PDE model is a linear system of hyperbolic PDEs, the numerical method will be validated on scalar first order hyperbolic PDEs whose solutions are known. Two such test problems will be:

$$\begin{aligned}
 u_t + au_x &= 0 \\
 u_t + u_x + u_y &= 0
 \end{aligned}
 \tag{15}$$

## 5 Testing

Testing will be conducted in two stages. Stage one will include applying the PDE numerical method to solve the CML PDE model. Simulations will first be run on the nonleukemic cell population to determine the validity of the scheme in relation to the proposed biological model. The appropriate alterations will then be made to the base model in order to achieve simulation of all three cell populations. Testing in this stage will conclude with numerical simulations of the entire system, resulting in figures similar to those presented by Kim *et al.* Validity will be determined by this model's ability to capture the CML behavior (fig. 5 and 6). This will be done in a manner similar to validation of the difference equation method.

Stage two of testing will be to determine whether these models can accurately depict CML genesis in a new set of patients. Simulations will be run with new parameter values that reflect clinical data of a different set of CML patients undergoing Imatinib treatment. This data originates from Dr. Frank Nicolini in Lyon, France. Dr. Nicolini is a collaborator of the project advisor. Figures of these simulations will be plotted for comparison.

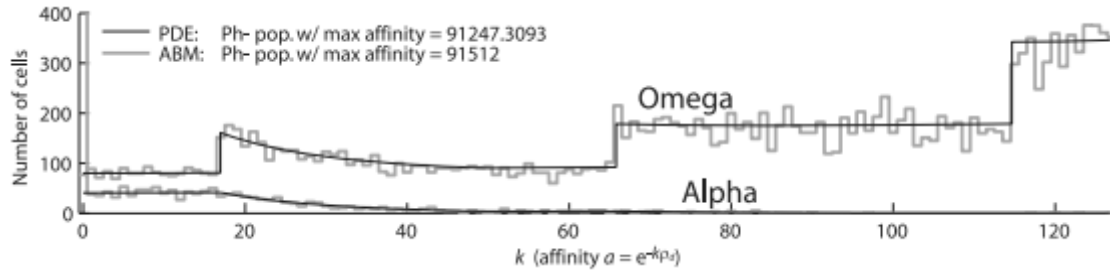


**Figure 5:** Steady state profile of nonleukemic cell population achieved by ABM and PDE model. Both resting and proliferating stem cell populations are shown. From [3].

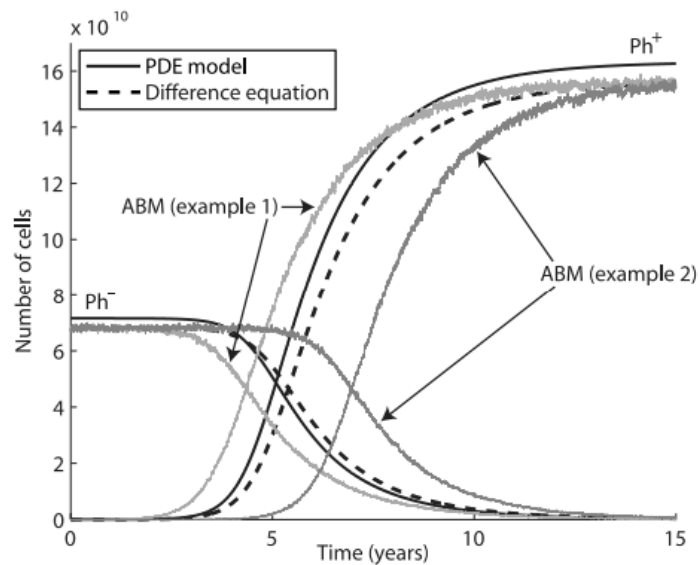


**Figure 6:** CML genesis as simulated by each of the three models. Dynamics of both leukemic ( $Ph^+$ ) and nonleukemic ( $Ph^-$ ) cells are shown by plotting the number of mature cells in each population versus time. From [3].

## 6 Project Schedule and Milestones

The project is divided into four phases as described below.

*Phase 1: October – mid-November*

- Implement difference equation model
- Improve efficiency and validate

*Phase 2: November – mid-December*

- Implement ABM
- Improve efficiency and validate

*Phase 3: December – mid-February*

- Implement basic PDE method
- Validate on simple test problem

*Phase 4: mid-February – April*

- Apply basic method to CML - Imatinib biology and validate
- Test models with clinical data
- Draw conclusions

## 7 Deliverables

Deliverables for this project will consist of Matlab code to simulate CML and its treatment according to the proposed models, a database or table of parameter values and initial conditions, and figures produced during simulations. Course requirements such as mid and end of year reports will also be included.

## 8 Bibliography

- [1] Roeder, I., Horn, M., Glauche, I., Hochhaus, A., Mueller, M.C., Loeffler, M., 2006. Dynamic modeling of imatinib-treated chronic myeloid leukemia: functional insights and clinical implications. *Nature Medicine*. 12(10): pp. 1181-1184
- [2] Kim, P.S., Lee P.P., and Levy, D., 2008. Modeling imatinib-treated chronic myelogenous leukemia: reducing the complexity of agent-based models. *Bulletin of Mathematical Biology*. 70(3): pp. 728-744.
- [3] Kim, P.S., Lee P.P., and Levy, D., 2008. A PDE model for imatinib-treated chronic myelogenous leukemia. *Bulletin of Mathematical Biology*. 70: pp. 1994-2016.
- [4] National Cancer Institute: PDQ® Chronic Myelogenous Leukemia Treatment. Bethesda, MD: National Cancer Institute. Date last modified 9/21/2015. Available at: <http://www.cancer.gov/types/leukemia/patient/cml-treatment-pdq>.